NACA

RESEARCH MEMORANDUM

USE OF FENCES TO INCREASE UNIFORMITY OF BOUNDARY LAYER ON SIDE WALLS OF SUPERSONIC WIND TUNNELS

By Rudolph C. Haefeli

Lewis Flight Propulsion Laboratory
Cleveland, Ohio

NATIONAL ADVISORY COMMITTEE
FOR AERONAUTICS
WASHINGTON
July 16, 1952

NATIONAL ADVISORY COMMITTEE FOR AERONAUTICS

RESEARCH MEMORANDUM

USE OF FENCES TO INCREASE UNIFORMITY OF BOUNDARY LAYER ON SIDE WALLS OF SUPERSONIC WIND TUNNELS

By Rudolph C. Haefeli

SUMMARY

An investigation of the use of solid fences installed on the side walls of a supersonic wind tunnel to retard the development of transverse flow and thus to increase the uniformity of the side-wall boundary layer is reported. Beneficial results were obtained with fences which had depths of the order of the boundary-layer displacement thickness and which followed potential-flow streamlines through the nozzle. Reduction of the number of fences on each side wall from four to two eliminated their effectiveness.

INTRODUCTION

Because of the static-pressure gradient normal to the axis of two-dimensional supersonic nozzles, transverse velocity components are initiated which cause large deviations of the boundary-layer streamlines from potential-flow streamlines (reference 1). Immediately downstream of the throat the pressure is greater at the center line of the tunnel than at the contour walls; therefore the side-wall boundary-layer flow is deflected farther away from the center line than the potential flow (fig. 1). Farther downstream, but still near the throat in the nozzle, the pressure becomes less at the center line than at the contour walls; the boundary-layer flow along the side walls therefore turns toward the center line. This transverse flow continues to increase in magnitude downstream of the nozzle because of the secondary flows peculiar to noncircular ducts (reference 2). Therefore, except close to the throat, the low-energy air of the boundary layer is continually swept toward the center line of the side walls as the flow progresses downstream (fig. 1). As a result, the boundary layer grows more rapidly along the side-wall center line. This growth is more pronounced at higher Mach numbers because the transverse pressure gradient in the nozzle increases with the design Mach number of the nozzle.

Some experimental data obtained in reference 3 and unpublished investigations which illustrate this boundary-layer growth are shown in

figure 2, in which the displacement thickness δ^* is plotted at various distances from the side-wall center line. The data of figure 2(a) were obtained by cross-plotting data presented in reference 3. The coordinate x', used in figure 2(a) to indicate the relative separation of the axial stations, is zero at the center of the test rhombus. The data of figures 2(b) and 2(c), obtained in the Lewis 12- by 12-inch and 6- by 6-inch tunnels, respectively, have not previously been reported. These data clearly show the increase of center-line displacement thickness with distance from the throat and with Mach number for these tunnels. The cusps, at $z = 0$, are indicative of secondary flow normal to the side wall within the boundary layer at the center line (fig. 1). It is apparent that at high supersonic Mach numbers the displacement thickness may become an appreciable fraction of the cross-section dimensions of small tunnels.

Theoretical predictions of the growth of the boundary layer along the side walls are difficult because of the complexity of the equations required to describe the flow. The existence of secondary flow in straight noncircular channels is, however, proved in reference 4 by an application of the vorticity transfer theory. Additional analyses of three-dimensional boundary-layer flows are presented in references 5 to 7. A method for calculating turbulent boundary-layer growth in the presence of pressure gradients along streamlines is given in reference 8. An application of this method to supersonic nozzle flow, however, yields values of displacement thickness which are not as large along the side-wall center line as those obtained experimentally.

Although the phenomena of the large boundary-layer growth along the center line can be explained, as yet, only qualitatively, several experimental means for increasing the uniformity of the boundary layer and thus increasing the useful test-section area and the maximum size of test models have been proposed. One of these, the installation of solid fences along potential-flow streamlines within the side-wall boundary layer to retard the transverse flow, has been investigated in the NACA Lewis 6- by 6-inch tunnel. The results of this investigation are presented herein.

Apparatus

This investigation was conducted in the Lewis 6- by 6-inch hypersonic continuous-flow wind tunnel. Further information about this tunnel is given in reference 9. The instrumentation included a pitot-pressure probe and a static-pressure probe (fig. 3) which were used with a mercury manometer and a differential butylphthalate manometer, respectively, for determining Mach numbers. A set of four fences, curved to follow potential-flow streamlines, was made to be mounted

on the side walls of the tunnel (figs. 4 and 5). The depth of protrusion into the stream was initially chosen approximately equal to nine tenths of the boundary-layer thickness (0.9δ). Two sets of fences with depths approximately equal to the displacement thickness δ^* and to twice the displacement thickness $2\delta^*$ were also used. These depths were determined experimentally without the fences at two axial stations on the fence streamlines and interpolated linearly. The fences, made from one-eighth inch brass strips to compromise between thinness and rigidity, were set in milled grooves and fastened to the side walls with screws. The upstream ends of the fences were tapered to a point.

Operating Conditions

The tests were conducted with an inlet pressure of 125 ±3 pounds per square inch gage within two temperature ranges, 125° ±3° F and 193° ±13° F. The dew-point temperature was less than -10° F at atmospheric pressure. The flow emptied into an exhaust line where a pressure of between 2 and 3 inches of mercury absolute was maintained. The test-section Reynolds numbers (computed from pressures measured in the test-section) were 1.8 to 2.7×10^6 per foot at a nominal Mach number of 5.5. No significant changes in the boundary-layer profiles could be attributed to inlet conditions within the ranges of these tests.

RESULTS

Mach number profiles with and without the fences (depths based on 0.9δ) installed are compared in figure 6. The fences reduce the boundary-layer thickness near the side-wall center line ($z = 0$) and increase the boundary-layer thickness nearer the contour wall ($z = 1$). The uniformity of the side-wall boundary layer is therefore increased. In addition, the fences reduce the distortion of the profiles at $z = 0$. In figure 6(b) the data for $z = 1$ are not shown because the fences extended through this station.

The axial variations of displacement thickness δ^* and momentum thickness θ obtained from these and other Mach number profiles are shown in figures 7 and 8. Values of δ^* and θ for the profiles of figure 6 are given in table I. These data show again that the uniformity of the boundary layer is increased by the fences.

The effect on the boundary layer of the fences with depths based on δ^* and $2\delta^*$ was about the same as that of the fences with the intermediate depth of 0.9δ; consequently, data are presented only for the fences with depth of 0.9δ. The deepest of the three sets of fences (those of depth of $2\delta^*$), however, caused undesirable disturbances in

the stream. Although the effect of the width of the fences was not investigated, one might expect to reduce these disturbances by using thinner fences.

In order to determine whether the length of the fences beyond the last tunnel expansion waves had an effect on this uniformity of the boundary layer, the fences with depths based on δ^* were shortened so that they extended only slightly into the test rhombus (downstream end indicated by X in fig. 4). These fences were as effective as the original fences in increasing the boundary-layer uniformity.

With the two internal or with the two external fences (depths based on 0.98) alternately removed there was no significant improvement on the results obtained without fences.

CONCLUSION

Side-wall fences which follow potential-flow streamlines through the nozzle effectively retard the secondary flow and increase the uniformity of the boundary layer on the side walls of two-dimensional supersonic tunnels. These fences need have depths no greater than the displacement thickness. The number of fences installed on each side wall affects the extent to which the secondary flow is retarded.

Lewis Flight Propulsion Laboratory
National Advisory Committee for Aeronautics
Cleveland, Ohio

REFERENCES

1. Brinich, Paul F.: Boundary-Layer Measurements in 3.84- by 10-Inch Supersonic Channel. NACA TN 2203, 1950.

2. Goldstein, Sidney: Modern Developments in Fluid Dynamics. Vols. I and II. Clarendon Press (Oxford), 1938, pp. 358-360.

3. Bollay, W.: Aerodynamics of Supersonic Aircraft and Missiles. Symposium on Ordnance Aeroballistics (Maryland), NOLR 1131, June 28, 1949, pp. 27-51.

4. Howarth, L.: Concerning Secondary Flow in Straight Pipes. Proc. Camb. Phil. Soc., vol. 34, pt. 3, July, 1938, pp. 335-344.

5. Moore, Franklin K.: Three-Dimensional Compressible Laminar Boundary-Layer Flow. NACA TN 2279, 1951.

6. Moore, Franklin K.: Displacement Effect of a Three-Dimensional Boundary-Layer. NACA TN 2722, 1952.

7. Mager, Artur: Generalization of Boundary-Layer Momentum-Integral Equations to Three-Dimensional Flows Including Those of Rotating System. NACA TN 2310, 1951.

8. Tucker, Maurice: Approximate Calculation of Turbulent Boundary-Layer Development in Compressible Flow. NACA TN 2337, 1951.

9. Bloom, Harold L.: Preliminary Survey of Boundary-Layer Development at a Nominal Mach number of 5.5. NACA RM E52D03, 1952.

TABLE I - VALUES OF DISPLACEMENT THICKNESS

AND MOMENTUM THICKNESS FOR PROFILES

OF FIGURE 6

Distance from throat (in.)	Without fences				With fences			
	Distance from side-wall center line, z, in.							
	0		1		0		1	
	δ^*	θ	δ^*	θ	δ^*	θ	δ^*	θ
16	0.50	0.034	0.14	0.010	0.34	0.022	----	-----
$27\frac{1}{2}$	.73	.052	.22	.016	.49	.034	0.48	0.033
$38\frac{1}{2}$	.88	.057	.22	.013	.63	.040	.54	.035
$49\frac{1}{2}$	.94	.068	.34	.024	.65	.042	.44	.029

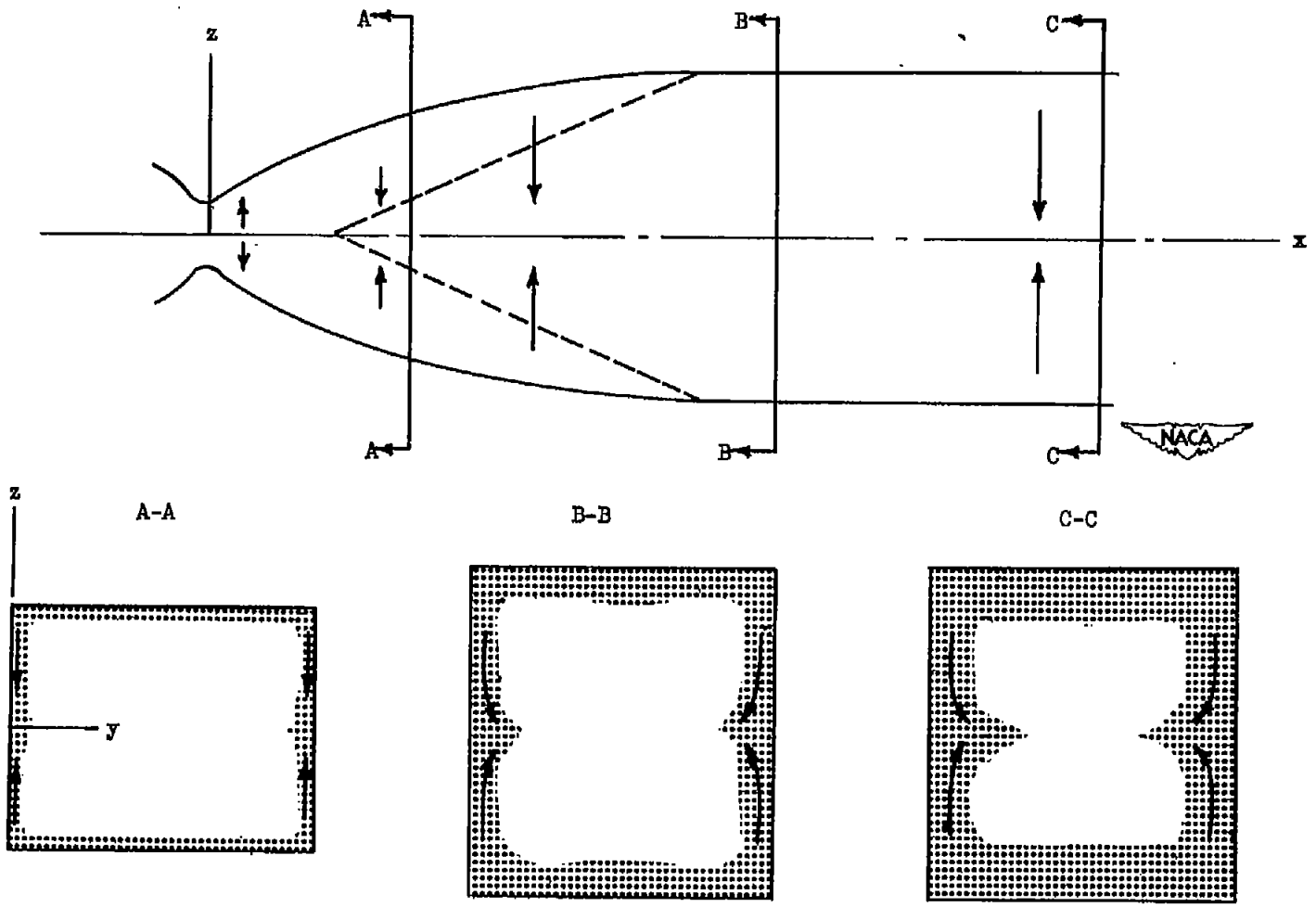

Figure 1. - Schematic diagram illustrating growth of boundary layer on tunnel walls. Arrows indicate direction of secondary flow; shaded area indicates boundary-layer region. Coordinate system is also shown.

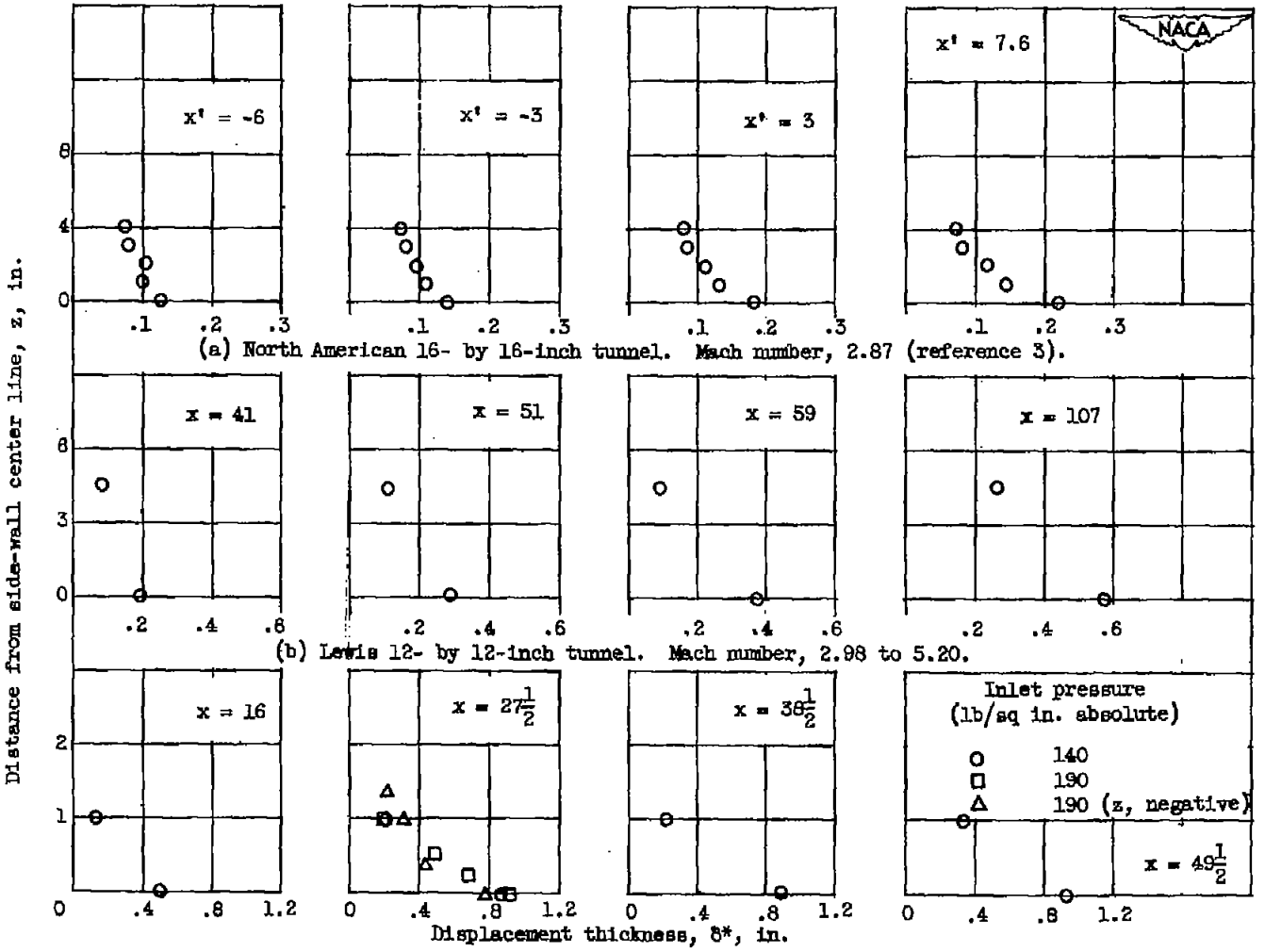

(a) North American 16- by 16-inch tunnel. Mach number, 2.87 (reference 3).

(b) Lewis 12- by 12-inch tunnel. Mach number, 2.98 to 5.20.

(c) Lewis 6- by 6-inch tunnel. Mach number, 5.2 to 5.7.

Figure 2. - Displacement thickness measured on side walls of three tunnels. x, distance from throat, in.; x', distance from center of test rhombus, in.

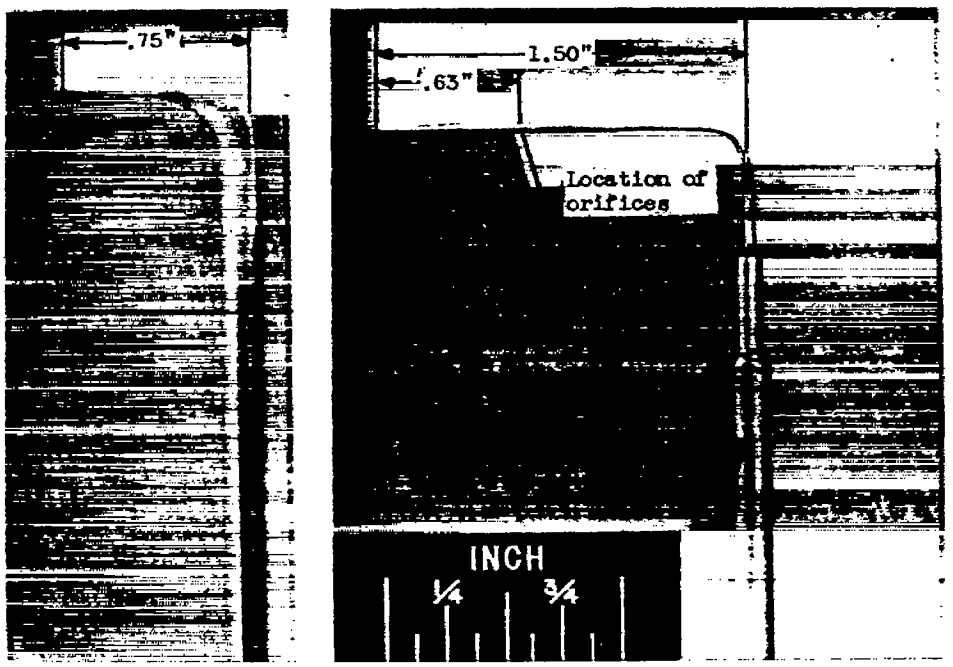

(a) Side views of pitot- and static-pressure probes.

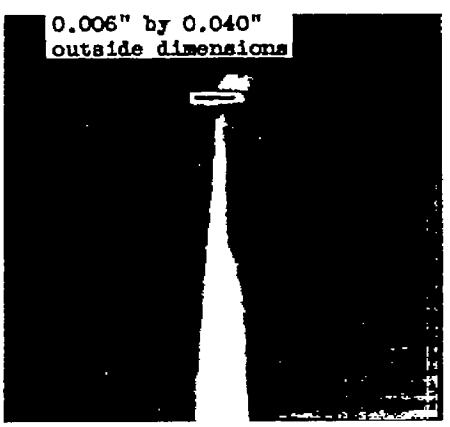

NACA
C-29724

(b) Front view of pitot-pressure probe (magnified).

Figure 3. - Pitot- and static-pressure survey probes.

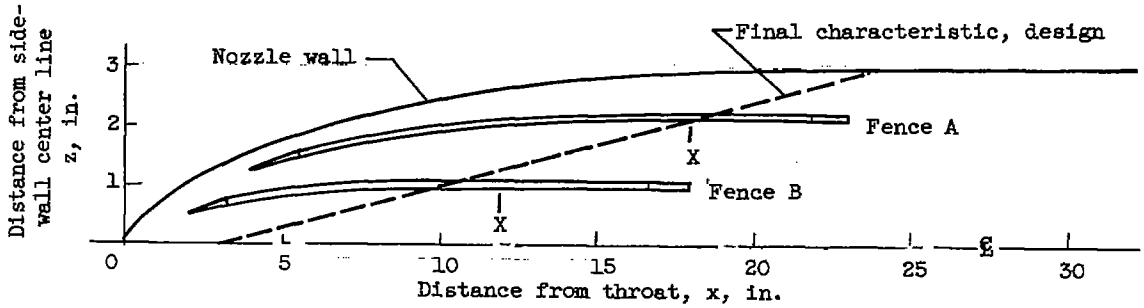

(a) Location of fences relative to tunnel nozzle.

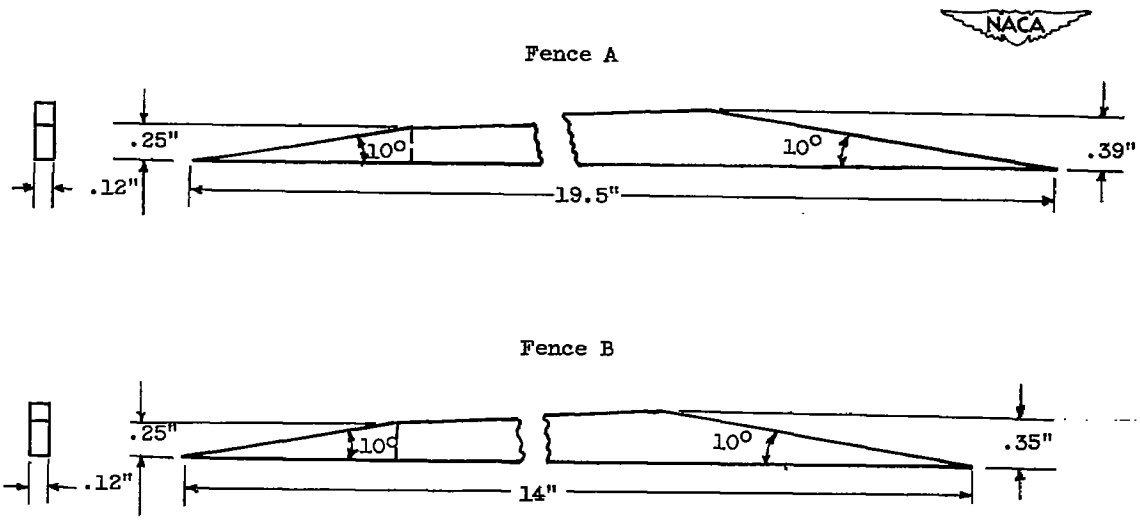

(b) Dimensions of fences with depths based on nine tenths of boundary-layer thickness.

Figure 4. - Geometry of fence installation.

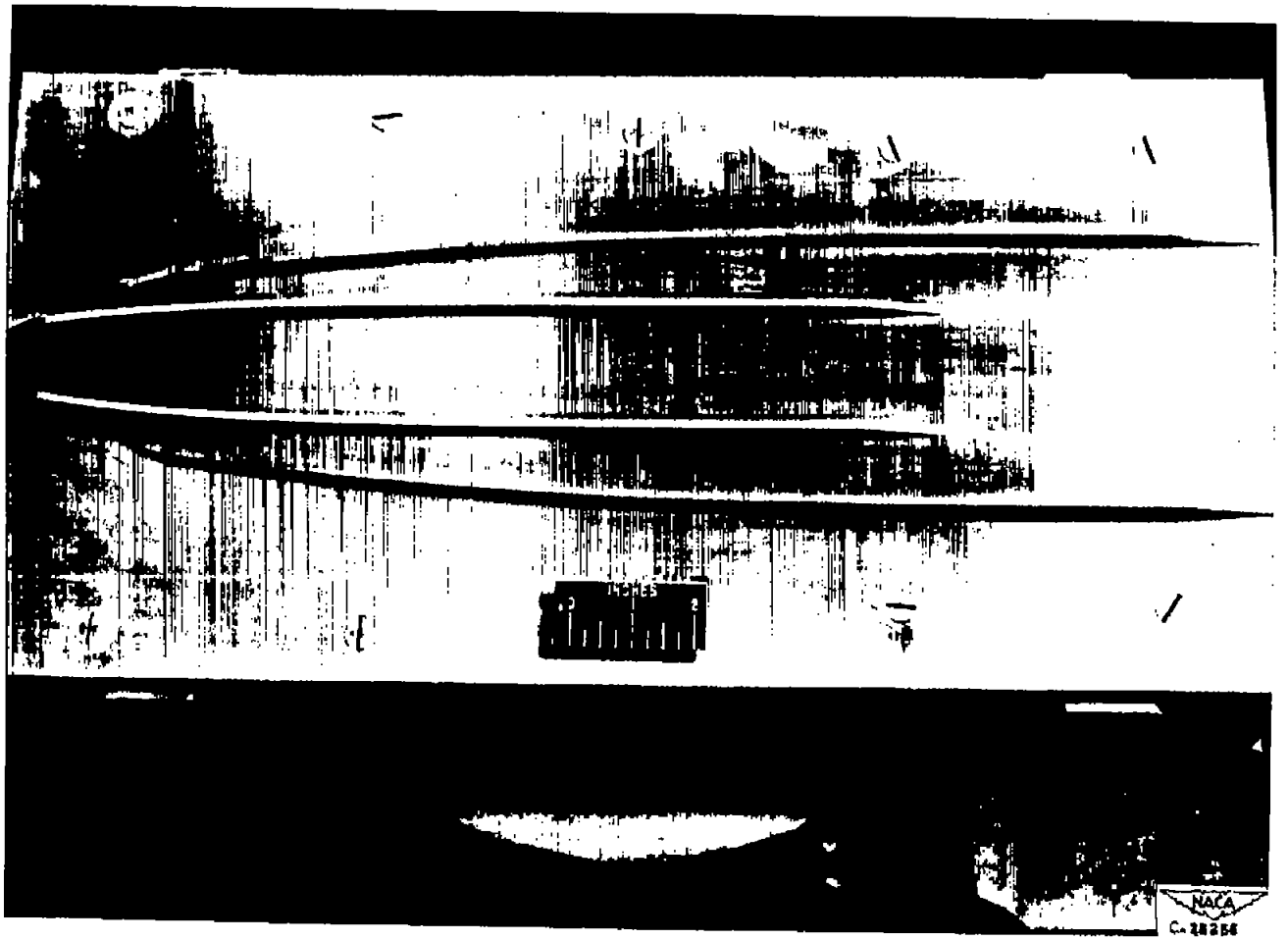

Figure 5. - Installation of fences on side wall.

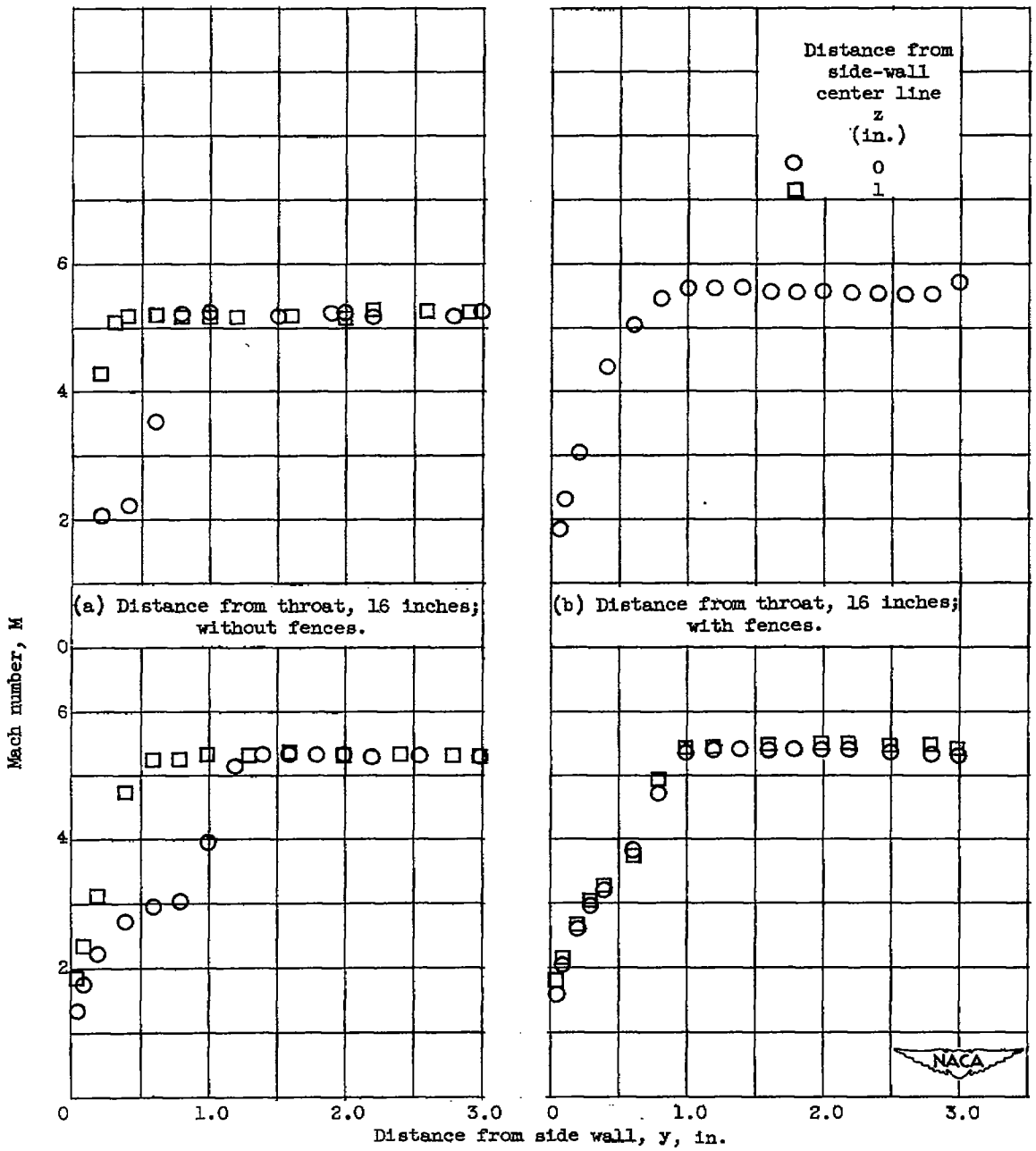

Figure 6. - Comparison of Mach number profiles at various axial distances from throat with and without fences.

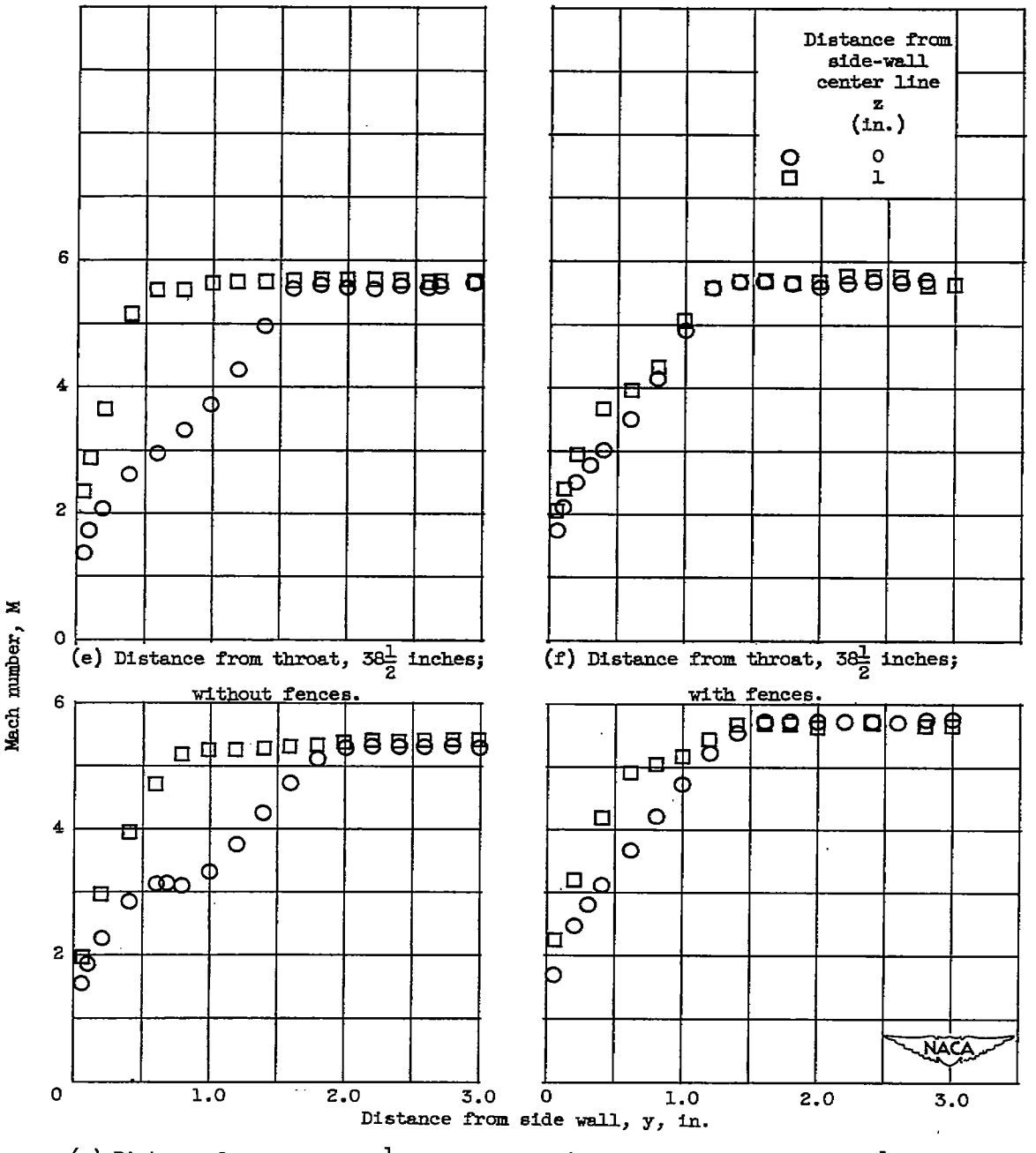

(e) Distance from throat, $38\frac{1}{2}$ inches; without fences.

(f) Distance from throat, $38\frac{1}{2}$ inches; with fences.

(g) Distance from throat, $49\frac{1}{2}$ inches; without fences.

(h) Distance from throat, $49\frac{1}{2}$ inches; with fences.

Figure 6. - Concluded. Comparison of Mach number profiles at various axial distances from throat with and without fences.

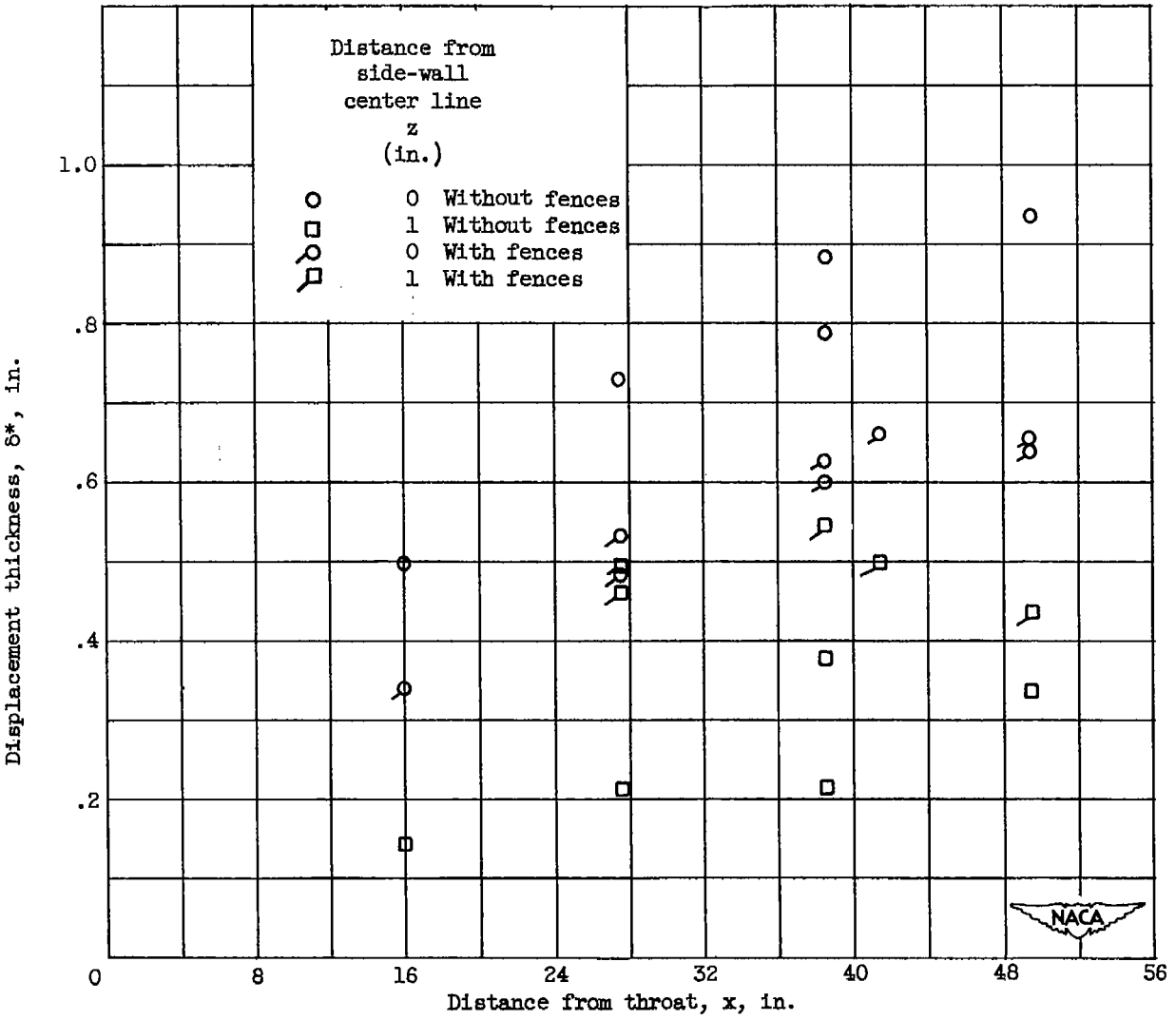

Figure 7. - Variation of displacement thickness with distance from throat.

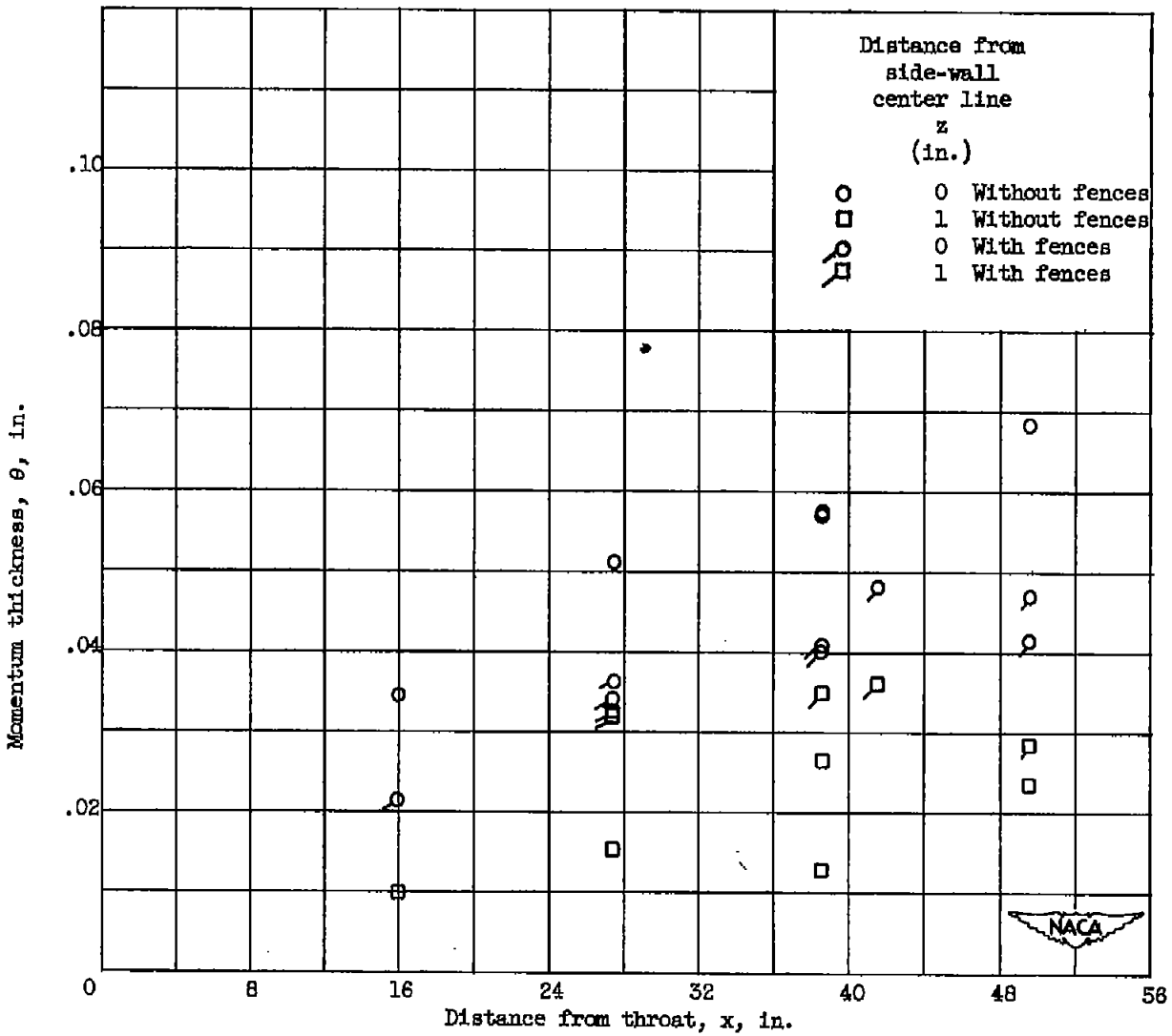

Figure 8. - Variation of momentum thickness with distance from throat.